

The “96 GeV excess” at the ILC

T. Biekötter

DESY, Notkestrasse 85, D-22607 Hamburg, Germany

M. Chakraborti

IFT (UAM/CSIC), Universidad Autónoma de Madrid, Cantoblanco, E-28048, Spain

S. Heinemeyer

*IFT (UAM/CSIC), Universidad Autónoma de Madrid Cantoblanco, E-28048, Spain
Campus of International Excellence UAM+CSIC, Cantoblanco, E-28049, Madrid, Spain
Instituto de Física de Cantabria (CSIC-UC), E-39005 Santander, Spain*

The CMS collaboration reported an intriguing $\sim 3\sigma$ (local) excess at 96 GeV in the light Higgs-boson search in the diphoton decay mode. This mass coincides with a $\sim 2\sigma$ (local) excess in the $b\bar{b}$ final state at LEP. We present the interpretation of this possible signal as the lightest Higgs boson in the 2 Higgs Doublet Model with an additional real Higgs singlet (N2HDM). It is shown that the type II and type IV (flipped) of the N2HDM can perfectly accommodate both excesses simultaneously, while being in agreement with all experimental and theoretical constraints. The excesses are most easily accommodated in the type II N2HDM, which resembles the Yukawa structure of supersymmetric models. We discuss the experimental prospects for constraining our explanation at future e^+e^- colliders, with concrete analyses based on the ILC prospects.

1 Introduction

The Higgs boson discovered in 2012 by ATLAS and CMS^{1,2} is so far consistent with the existence of a Standard-Model (SM) Higgs boson³ with a mass of ~ 125 GeV. However, the experimental uncertainties on the Higgs-boson couplings are (if measured already) at the precision of $\sim 20\%$, so that there is room for Beyond Standard-Model (BSM) interpretations. Many theoretically well motivated extensions of the SM contain additional Higgs bosons. In particular, the presence of Higgs bosons lighter than 125 GeV is still possible.

Searches for light Higgs bosons have been performed at LEP, the Tevatron and the LHC. Besides the SM-like Higgs boson at 125 GeV no further detections of scalar particles have been reported. However, two excesses have been seen at LEP and the LHC at roughly the same mass, hinting to a common origin of both excesses via a new particle state. LEP observed a 2.3σ local excess in the $e^+e^- \rightarrow Z(H \rightarrow b\bar{b})$ searches⁴, consistent with a scalar of mass ~ 98 GeV, where the mass resolution is rather imprecise due to the hadronic final state. The signal strength was extracted to be $\mu_{\text{LEP}} = 0.117 \pm 0.057$. The signal strength μ_{LEP} is the measured cross section normalized to the SM expectation assuming a SM Higgs-boson mass at the same mass.

CMS searched for light Higgs bosons in the diphoton final state. Run II⁵ results show a local excess of $\sim 3\sigma$ at ~ 96 GeV, and a similar excess of 2σ at roughly the same mass⁶ in Run I. Assuming dominant gluon fusion production the excess corresponds to $\mu_{\text{CMS}} = 0.6 \pm 0.2$. First Run II results from ATLAS with 80 fb^{-1} in the diphoton final state turned out to be weaker than the corresponding CMS results, see, e.g., Fig. 1 in⁷. Possibilities are discussed in the literature of how to simultaneously explain both excesses by a common origin. In particular

^aTalk presented at the International Workshop on Future Linear Colliders (LCWS2019), Sendai, Japan, 28 October-1 November, 2019. C19-10-28.

supersymmetric realizations can be found in ^{8,9,10,11,12,13}. For a review we refer to Refs. ^{14,7}, see also Ref. ¹⁵.

2 The N2HDM

We discussed in ^{16,17} how a ~ 96 GeV Higgs boson of the Next to minimal 2 Higgs Doublet Model (N2HDM) ^{18,19} can be the origin of both excesses in the type II and type IV scenarios. The N2HDM extends the CP-conserving 2 Higgs Doublet Model (2HDM) by a real scalar singlet field. In analogy to the 2HDM, a Z_2 symmetry is imposed to avoid flavor changing neutral currents at the tree level, which is only softly broken in the Higgs potential. Furthermore, a second Z_2 symmetry, under which the singlet field changes the sign, constraints the scalar potential. This symmetry is broken spontaneously during electroweak symmetry breaking (EWSB), as soon as the singlet field obtains a vacuum expectation value (vev).

In total, the Higgs sector of the N2HDM consists of 3 CP-even Higgs bosons h_i , 1 CP-odd Higgs boson A , and 2 charged Higgs bosons H^\pm . In principle, each of the particles h_i can account for the SM Higgs boson at 125 GeV. In our analysis, h_2 will be identified with the SM Higgs boson, while h_1 plays the role of the potential state at ~ 96 GeV. The third CP-even and the CP-odd states h_3 and A were assumed to be heavier than 400 GeV to avoid LHC constraints. The charged Higgs-boson mass was set to be larger than 650 GeV to satisfy constraints from flavor physics observables.

In the physical basis the 12 independent parameters of the model are the mixing angles in the CP-even sector $\alpha_{1,2,3}$, the ratio of the vevs of the Higgs doublets $\tan \beta = v_2/v_1$, the SM vev $v = \sqrt{v_1^2 + v_2^2}$, the vev of the singlet field v_S , the masses of the physical Higgs bosons $m_{h_{1,2,3}}$, m_A and M_{H^\pm} , and the soft Z_2 breaking parameter m_{12}^2 . Using the public code `ScannerS` ^{20,19} we performed a scan over the following parameter ranges:

$$\begin{aligned} 95 \text{ GeV} \leq m_{h_1} \leq 98 \text{ GeV} , \quad m_{h_2} = 125.09 \text{ GeV} , \quad 400 \text{ GeV} \leq m_{h_3} \leq 1000 \text{ GeV} , \\ 400 \text{ GeV} \leq m_A \leq 1000 \text{ GeV} , \quad 650 \text{ GeV} \leq M_{H^\pm} \leq 1000 \text{ GeV} , \\ 0.5 \leq \tan \beta \leq 4 , \quad 0 \leq m_{12}^2 \leq 10^6 \text{ GeV}^2 , \quad 100 \text{ GeV} \leq v_S \leq 1500 \text{ GeV} . \end{aligned} \quad (1)$$

The following experimental and theoretical constraints were taken into account:

- tree-level perturbativity, boundedness-from-below and global-minimum conditions
- Cross-section limits from collider searches using `HiggsBounds v.5.3.2` ^{21,22,23,24}
- Signal-strength measurements of the SM Higgs boson using `HiggsSignals v.2.2.3` ^{25,26,27}
- Various flavor physics observables, in particular excluding $M_{H^\pm} < 650$ GeV for all values of $\tan \beta$ in the type II and IV.
- Electroweak precision observables in terms of the oblique parameters S , T and U ^{28,29}

For more details we refer to Ref. ¹⁶. The relevant input for `HiggsBounds` and `HiggsSignals`, (decay widths, cross sections), were obtained using the public codes `N2HDECAY` ^{19,30} and `SusHi` ^{31,32}.

3 Implications for future e^+e^- colliders

The results of our parameter scans in the type II and type IV N2HDM, as given in ¹⁶, show that both types of the N2HDM can accommodate the excesses simultaneously, while being in agreement with all considered constraints described above. A preference of larger values of μ_{CMS} in the type II scenario is visible, which is caused by the suppression of decays into τ -pairs (see ¹⁶ for details).

The particle h_1 is dominantly singlet-like, and acquires its coupling to the SM particles via the mixing with the SM Higgs boson h_2 . Thus, the presented scenario will be experimentally accessible in two complementary ways. Firstly, the new particle h_1 can be produced directly in collider experiments. Secondly, deviations of the couplings of 125 GeV Higgs boson h_2 from the

SM predictions are present. We propose experimental analyses to constrain (or confirm) our explanation of the excesses, both making use of the two effects mentioned above.

3.1 Precision Higgs measurements: HL-LHC vs. ILC

Due to the presence of the additional light Higgs boson which is substantially mixed with the SM Higgs boson, the scenario deviates from the well-known alignment limit of the 2HDM. Currently, uncertainties on the measurement of the coupling strengths of the SM-like Higgs boson at the LHC are still large, i.e., at the 1σ -level they are of the same order as the modifications of the couplings present in our analysis in the N2HDM^{3,33,34}. In the future tighter constraints are expected from the LHC after the high-luminosity upgrade (HL-LHC), when the planned amount of 3000 fb^{-1} integrated luminosity will have been collected³⁵. Finally, a future linear e^+e^- collider like the ILC could improve the precision measurements of the Higgs boson couplings even further^{35,36}^b. We compare our scan points to the expected precisions of the LHC and the ILC as they are reported in Refs.^{37,38}, neglecting possible correlations of the coupling modifiers.

In Fig. 1 we plot the coupling modifier of the SM-like Higgs boson h_2 to τ -leptons, $c_{h_2\tau\tau}$ on the horizontal axis against the coupling coefficient to b -quarks, $c_{h_2b\bar{b}}$ (top), to t -quarks, $c_{h_2t\bar{t}}$ (middle) and to the massive SM gauge bosons, c_{h_2VV} (bottom), for both types. These points passed all the experimental and theoretical constraints, including the verification of SM-like Higgs boson properties in agreement with LHC results using `HiggsSignals`. In the top plot the blue points lie on a diagonal line, because in type II the coupling to leptons and to down-type quarks scale identically, while in the bottom plot the red points representing the type IV scenario lie on the diagonal, because there the lepton-coupling scales in the same way as the coupling to up-type quarks. The current measurements on the coupling modifiers by ATLAS³³ and CMS³⁴ are shown as black ellipses, although the corresponding uncertainties are still very large.

We include several future precisions for the coupling measurements. It should be noted that they are centered around the SM predictions to show the potential to discriminate the SM from the N2HDM. The magenta ellipse in each plot shows the expected precision of the measurement of the coupling coefficients at the 1σ -level at the HL-LHC from Ref.³⁸. The current uncertainties and the HL-LHC analysis are based on the coupling modifier, or κ -framework. These modifiers are then constrained using a global fit to projected HL-LHC data assuming no deviation from the SM prediction will be found. We use the uncertainties given under the assumptions that no decay of the SM-like Higgs boson to BSM particles is present, and that current systematic uncertainties will be reduced in addition to the reduction of statistical uncertainties due to the increased statistics.

The green and the orange ellipses show the corresponding expected uncertainties when the HL-LHC results are combined with projected data from the ILC after the 250 GeV phase and the 500 GeV phase, respectively, taken from Ref.³⁷. Their analysis is based on a pure effective field theory calculation, supplemented by further assumptions to facilitate the combination with the HL-LHC projections in the κ -framework. In particular, in the effective field theory approach the vector boson couplings can be modified beyond a simple rescaling. This possibility was excluded by recasting the fit setting two parameters related to the couplings to the Z -boson and the W -boson to zero (for details we refer to Ref.³⁷).

While current constraints on the SM-like Higgs-boson properties allow for large deviations of the couplings of up to 40%, the allowed parameter space of our scans will be significantly reduced by the expected constraints from the HL-LHC and the ILC.^c For instance, the uncertainty of the coupling to b -quarks will shrink below 4% at the HL-LHC and below 1% at the ILC. For the coupling to τ -leptons the uncertainty is expected to be at 2% at the HL-LHC. Again, the ILC could reduce this uncertainty further to below 1%. For the coupling to t -quarks, on the

^bSimilar results can be obtained for CLIC, FCC-ee and CEPC. We will focus on the ILC prospects here using the results of Ref.³⁶.

^cHere one has to keep in mind the theory input required in the (HL-)LHC analysis.

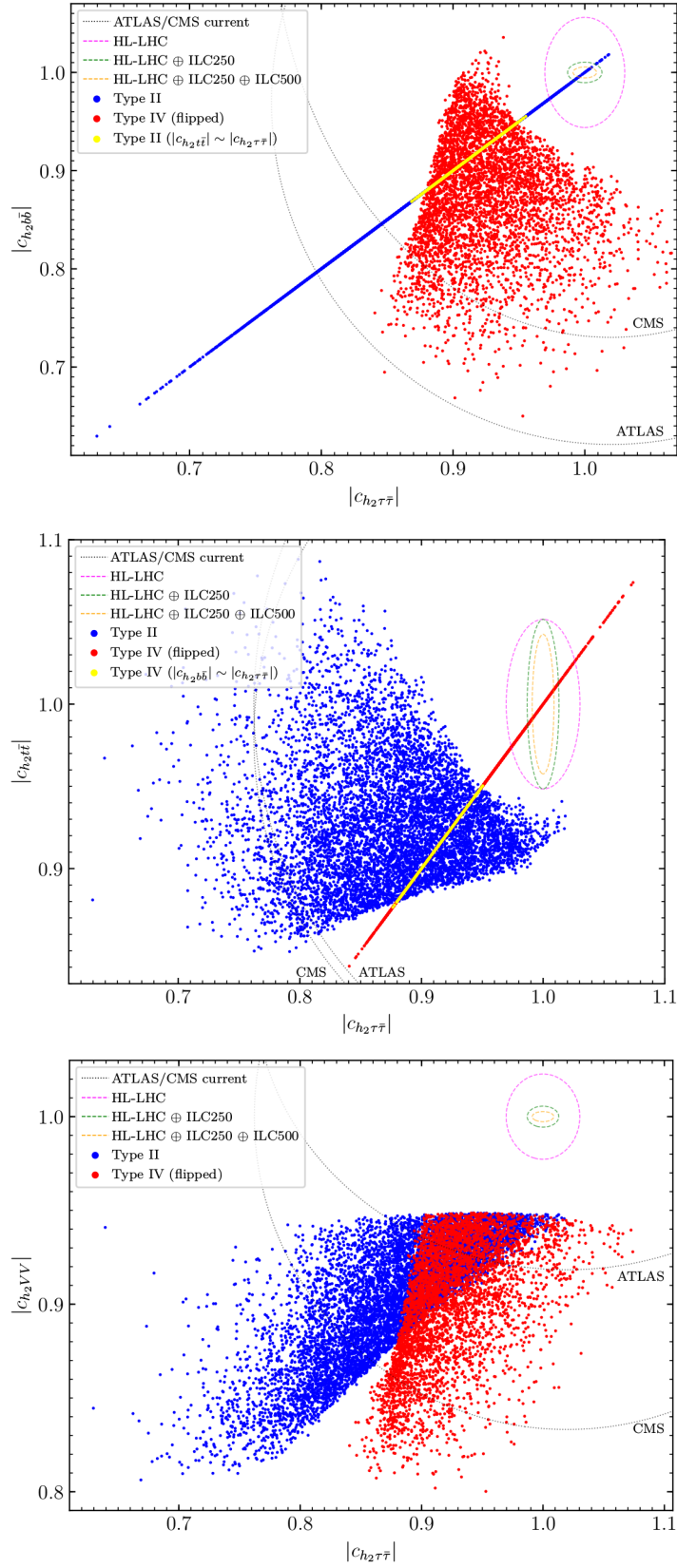


Figure 1 – Prospects for the Higgs coupling measurements at the HL-LHC and the ILC (see text). The upper, middle and lower plot show the planes of $|c_{h_2 \tau \tau}| - |c_{h_2 t \bar{t}}|$, $|c_{h_2 \tau \tau}| - |c_{h_2 b \bar{b}}|$, $|c_{h_2 \tau \tau}| - |c_{h_2 V V}|$.

other hand, the ILC cannot substantially improve the expected uncertainty of the HL-LHC (but permit a model-independent analysis). Still, the HL-LHC and the ILC are expected to reduce the uncertainty by roughly a factor of three. This demonstrates that our explanation of the LEP and the CMS excesses within the N2HDM is testable indirectly using future precision measurements of the SM-like Higgs-boson couplings.

Comparing the top and middle plots in Fig. 1 we find that, independent of the type of the N2HDM, there is not a single benchmark point that coincides with the SM prediction regarding the three coupling coefficients shown. This implies that, once these couplings are measured precisely by the HL-LHC and the ILC, a deviation of the SM prediction has to be measured in at least one of the couplings, if our explanation of the excesses is correct. Conversely, if no deviation from the SM prediction regarding these couplings will be measured, our explanation would be ruled out entirely. Furthermore, in the case that a deviation from the SM prediction will be found, the predicted scaling behavior of the coupling coefficients in the type II scenario (upper plot) and the type IV scenario (middle plot), might lead to distinct possibilities for the two models to accommodate these possible deviations. In this case, precision measurements of the SM-like Higgs boson couplings could be used differentiate between the type II and type IV solution and thus to exclude one of the two scenarios. This is true for all points except the ones highlighted in yellow in Fig. 1. The yellow points are a subset of points of our scans that, if such deviations of the SM-like Higgs boson couplings will be measured, could correspond to a benchmark point both in the type II and type IV.

Finally, in the lower plot of Fig. 1, where the absolute value of the coupling modifier of the SM-like Higgs boson w.r.t. the vector boson couplings $|c_{h_2VV}|$ is shown on the vertical axis, the parameter points of both types show deviations larger than the projected experimental uncertainty at HL-LHC and ILC. The deviations in $|c_{h_2VV}|$ are even stronger than for the couplings to fermions. A 2σ deviation from the SM prediction is expected with HL-LHC accuracy. At the ILC a deviation of more than 5σ would be visible. As mentioned already, a suppression of the coupling to vector bosons is explicitly expected by demanding $\Sigma_{h_2} \geq 10\%$. However, since points with lower singlet component cannot accommodate both excesses, this does not contradict the conclusion that the explanation of both excesses can be probed with high significance with future Higgs-boson coupling measurements.

3.2 Production of the 96 GeV Higgs at the ILC

Regarding future collider experiments beyond the LHC, a lepton collider is expected to be able to produce and analyse the additional light Higgs boson h_1 . As an example, we compare the current LEP bounds and the prospects of the International Linear Collider (ILC), based on³⁶, to our scan points in the type II scenario in Fig. 2 (left). We show the expected 95% CL upper limits at the ILC using the traditional (red) and the recoil technique (green)³⁶. We indicate the points which lie within (blue) and outside (red) the 1σ ellipse regarding μ_{LEP} and μ_{CMS} . Remarkably, all the points we found that fit the LEP and the CMS excesses at the 1σ level would be excluded by the ILC, if no deviations from the SM background would be observed. On the other hand, if the 96 GeV Higgs boson is realized in nature, the ILC would be able to produce it in large numbers.

Acknowledgements

The work was supported in part by the MEINCOP (Spain) under contract FPA2016-78022-P and in part by the AEI through the grant IFT Centro de Excelencia Severo Ochoa SEV-2016-0597. The work of S.H. was supported in part by the Spanish Agencia Estatal de Investigación (AEI), in part by the EU Fondo Europeo de Desarrollo Regional (FEDER) through the project FPA2016-78645-P, in part by the ‘‘Spanish Red Consolider MultiDark’’ FPA2017-90566-REDC.

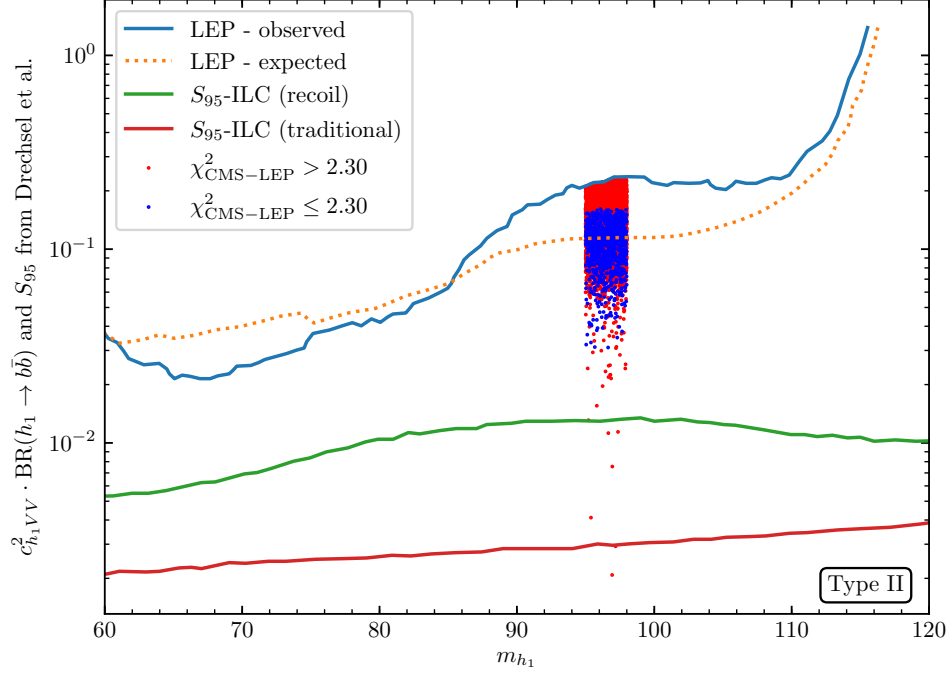


Figure 2 – The 95% CL expected (orange dashed) and observed (blue) upper bounds on the Higgsstrahlung production process with associated decay of the scalar to a pair of bottom quarks at LEP⁴. The expected ILC sensitivities are given by the green and red line (see text)³⁶. N2HDM type II model points within (outside) the 1σ CL of the 96 GeV excess are shown as blue (red) dots. N2HDM type IV results are similar.

T.B. is supported by the Deutsche Forschungsgemeinschaft under Germany’s Excellence Strategy EXC2121 “Quantum Universe” - 390833306.

References

1. Georges Aad et al. *Phys. Lett.*, B716:1–29, 2012.
2. Serguei Chatrchyan et al. *Phys. Lett.*, B716:30–61, 2012.
3. Georges Aad et al. *JHEP*, 08:045, 2016.
4. R. Barate et al. *Phys. Lett.*, B565:61–75, 2003.
5. Albert M Sirunyan et al. arXiv:1811.08459.
6. Technical Report CMS-PAS-HIG-14-037, 2015.
7. S. Heinemeyer and T. Stefaniak. arXiv:1812.05864.
8. T. Biekotter, S. Heinemeyer, and C. Munoz. *Eur. Phys. J.*, C78(6):504, 2018.
9. F. Domingo, S. Heinemeyer, S. Paßehr, and G. Weiglein. *Eur. Phys. J.*, C78(11):942, 2018.
10. W. G. Hollik, S. Liebler, G. Moortgat-Pick, S. Paßehr, and G. Weiglein. *Eur. Phys. J.*, C79(1):75, 2019.
11. Kiwoon Choi, Sang Hui Im, Kwang Sik Jeong, and Chan Beom Park. *Eur. Phys. J.*, C79(11):956, 2019.
12. T. Biekotter, S. Heinemeyer, and C. Muñoz. *Eur. Phys. J.*, C79(8):667, 2019.
13. Junjie Cao, Xinglong Jia, Yuanfang Yue, Haijing Zhou, and Pengxuan Zhu. 2019.
14. S. Heinemeyer. *Int. J. Mod. Phys.*, A33(31):1844006, 2018.
15. Francois Richard. arXiv:2001.04770.
16. T. Biekotter, M. Chakraborti, and S. Heinemeyer. arXiv:1903.11661.
17. Thomas Biekotter, M. Chakraborti, and Sven Heinemeyer. arXiv:1905.03280.
18. Chien-Yi Chen, Michael Freid, and Marc Sher. *Phys. Rev.*, D89(7):075009, 2014.

19. M. Muhlleitner, M. O. P. Sampaio, R. Santos, and J. Wittbrodt. *JHEP*, 03:094, 2017.
20. Rita Coimbra, Marco O. P. Sampaio, and Rui Santos. *Eur. Phys. J.*, C73:2428, 2013.
21. P. Bechtle, O. Brein, S. Heinemeyer, G. Weiglein, and K. Williams. *Comput. Phys. Commun.*, 181:138–167, 2010.
22. P. Bechtle, O. Brein, S. Heinemeyer, G. Weiglein, and K. Williams. *Comput. Phys. Commun.*, 182:2605–2631, 2011.
23. P. Bechtle, O. Brein, S. Heinemeyer, O. Stål, T. Stefaniak, G. Weiglein, and K. Williams. *Eur. Phys. J.*, C74(3):2693, 2014.
24. P. Bechtle, S. Heinemeyer, O. Stål, T. Stefaniak, and G. Weiglein. *Eur. Phys. J.*, C75(9):421, 2015.
25. P. Bechtle, S. Heinemeyer, O. Stål, T. Stefaniak, and G. Weiglein. *Eur. Phys. J.*, C74(2):2711, 2014.
26. Oscar Stål and Tim Stefaniak. *PoS*, arXiv:1310.4039.
27. P. Bechtle, S. Heinemeyer, O. Stål, T. Stefaniak, and G. Weiglein. *JHEP*, 11:039, 2014.
28. Michael E. Peskin and Tatsu Takeuchi. *Phys. Rev. Lett.*, 65:964–967, 1990.
29. Michael E. Peskin and Tatsu Takeuchi. *Phys. Rev.*, D46:381–409, 1992.
30. A. Djouadi, J. Kalinowski, and M. Spira. *Comput. Phys. Commun.*, 108:56–74, 1998.
31. R. Harlander, S. Liebler, and H. Mantler. *Comput. Phys. Commun.*, 184:1605, 2013.
32. R. Harlander, S. Liebler, and H. Mantler. *Comput. Phys. Commun.*, 212:239, 2017.
33. Technical Report ATLAS-CONF-2018-031, Jul 2018.
34. Albert M Sirunyan et al. *Eur. Phys. J.*, C79(5):421, 2019.
35. Sally Dawson et al. arXiv:1310.8361.
36. P. Drechsel, G. Moortgat-Pick, and G. Weiglein. arXiv:1801.09662.
37. Philip Bambade et al. arXiv:1903.01629.
38. M. Cepeda et al. arXiv:1902.00134.